Phase contrast and susceptibility mapping in the mouse abdomen at 7T for super-paramagnetic particle visualization

Dávid Z. Balla[1], Jörn Engelmann[1], Sven Gottschalk[1], Klaus Scheffler[1,2], Rolf Pohmann[1]
1) Max Planck Institute for Biological Cybernetics, Tübingen, Germany, 2) Department of Biomedical Magnetic Resonance, University of Tübingen, Germany

Introduction:

The phase of the MR-signal contains useful information about the local and temporal variations of the magnetic field. Structural phase imaging in the brain reveals a contrast, which is not available in the modulus intensity maps and serves as a complementary source of information to conventional MRI (1). Quantitative susceptibility mapping (QSM) is a reconstruction technique, which deconvolves non-local effects from the phase distribution and unveils a major source of T2* and phase contrast, namely local tissue susceptibility (2,3). Both non-local phase contrast imaging and the QSM method have potential applications in the detection and quantification of super-paramagnetic particles in organs other than the brain. Therefore, we investigated the local phase contrast in the mouse abdomen at 7T with and without contrast agent and applied a QSM-algorithm originally developed for human brain applications on the phase images.

Materials & Methods:

Two adult male C57BL/6J mice were sacrificed and perfused first with phosphate buffer and afterwards with formalin for fixation, one of them 5 hours after intravenous injection of 1500µg of carbon-coated Cobalt nanoparticles suspended in 150µl PBS. Mice were imaged *ex vivo* in a Bruker 70/30 Biospec with a Tx/Rx quadrature birdcage coil with 40mm inner diameter. An isotropic resolution of 60µm³ was achieved with a T2*-weighted 3D-FLASH sequence. For the untreated mouse, TR=25ms, TE=10ms, α=20°, NA=22, and for the treated animal, TR=15ms, TE=5.5ms, α=8°, NA=36 were applied. Local phase contrast was calculated by high-pass filtering of the phase images using 2D Gaussian convolution with σ≤1mm. QSM was performed with a regularized L2-norm minimization algorithm, with the field perturbation maps (derived from the filtered phase images) as input, and the magnitude images as *a priori* knowledge for norm weighting (3,4).

Results:

A coronal slice containing the kidneys is selected in both datasets for demonstration (Fig. 1 and 2). In case of the untreated mouse, the magnitude images provide high structural detail clearly revealing organs like the liver, the kidneys and the pancreas (Fig.1a). In the treated animal, massive accumulation of the contrast agent in the liver and the spleen causes non-local signal cancellation in neighboring tissue (Fig.2a). This effect is more obvious in the phase image (Fig.1b and 2b). For filtering out strong non-local contributions (even spatial phase-wraps), an aggressive high-pass filter is needed, which reduces the structural contrast (Fig.1b). However, the local perturbations by single (not clustered) particles pass the filter and are easily discernible on the flattened background (Fig.2b, red arrows point to some of the sites where particle-contrast was detected). Susceptibility maps (χ) are shown in Fig. 1c and Fig. 2c revealing some diagonal reconstruction artifacts known from brain applications.

Discussion and Conclusions:

Here we have presented an application of phase imaging and QSM in the mouse abdomen at 7T. Dominant non-local phase effects had to be filtered out and, therefore, the native structural phase contrast in the abdomen was strongly reduced. The implication of this on particle-contrast, however, was not critical, suggesting that phase imaging in the abdomen can be useful for detection of single targeted particles in relatively homogeneous organs like the kidney, the pancreas or muscle tissue. In regions without spatial phase-wraps the tested QSM algorithm had similar performance as in the brain, providing quantitative maps of the local MRI-contrast source. For thinkable future applications the deconvolution of non-local effects in QSM could become an important aspect in addition to susceptibility quantification.

References: 1) Duyn et al. (2007) PNAS 104:11796. 2) Schaefer et al. (2008) ISMRM 641. 3) de Rochefort et al. (2008) 60:1003. 4) Wharton and Bowtell (2010) NeuroImage 53:515.

Figure 1

(a) (b) (c)

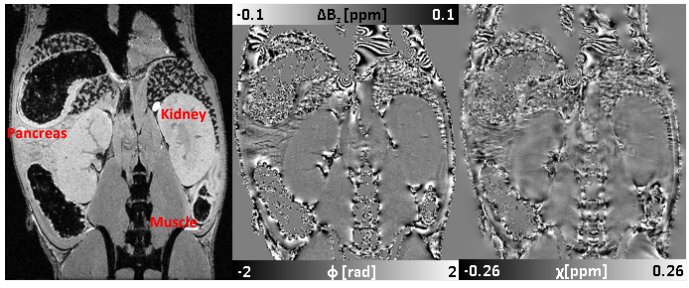

Figure 2

(a) (b) (c)